Electrically Driven Single-Photon Superradiance from Molecular Chains in a Plasmonic Nanocavity

Yang Luo,[1,*] Gong Chen,[1,2,*] Yang Zhang,[1,†] Li Zhang,[1] Yunjie Yu,[1] Fanfang Kong,[1] Xiaojun Tian,[1] Yao Zhang,[1] Chongxin Shan,[2] Yi Luo,[1] Jinlong Yang,[1] Vahid Sandoghdar,[3] Zhenchao Dong,[1,‡] and J. G. Hou[1,§]

[1]*Hefei National Laboratory for Physical Sciences at the Microscale and Synergetic Innovation Center of Quantum Information & Quantum Physics, University of Science and Technology of China, Hefei, Anhui 230026, China*

[2]*School of Physics and Engineering, Zhengzhou University, Zhengzhou 450052, China*

[3]*Max Planck Institute for the Science of Light, Erlangen 91058, Germany*

(Received 4 January 2019; published 12 June 2019)

We demonstrate single-photon superradiance from artificially constructed nonbonded zinc-phthalocyanine molecular chains of up to 12 molecules. We excite the system via electron tunneling in a plasmonic nanocavity and quantitatively investigate the interaction of the localized plasmon with single-exciton superradiant states resulting from dipole-dipole coupling. Dumbbell-like patterns obtained by subnanometer resolved spectroscopic imaging disclose the coherent nature of the coupling associated with superradiant states while second-order photon correlation measurements demonstrate single-photon emission. The combination of spatially resolved spectral measurements with theoretical considerations reveals that nanocavity plasmons dramatically modify the linewidth and intensity of emission from the molecular chains, but they do not dictate the intrinsic coherence of the superradiant states. Our studies shed light on the optical properties of molecular collective states and their interaction with nanoscopically localized plasmons.

DOI: 10.1103/PhysRevLett.122.233901

When N two-level emitters undergo dipole-dipole coupling, new collective states are formed as a result of quantum superposition of product states with well-defined phases [1–5]. Such coherent intermolecular dipole-dipole interactions can lead to various phenomena such as coherent energy transfer, photosynthesis, and new quantum engineered systems [6–10]. One of the interesting features of quantum coherent collective states is single-photon superradiance (SPS), namely, the generation of a singly excited symmetric collective state [1,11,12]. However, quantitative studies of SPS in molecular systems confront challenges concerning the precise control and characterization of intermolecular dipole-dipole coupling, including the number of coupled monomers (N), intermolecular distances, dipole arrangements and orientations, as well as their phase relations. Furthermore, it would be highly desirable to have optical access to each individual constituent of a molecular system such as a chain.

Scanning tunneling microscopy (STM) can be used with unprecedented control to assemble molecular chains and to study their electroluminescence properties [13,14], including single-photon emission [15,16]. Nanoscopic plasmonic antennas and cavities have been used in the past decade to enhance absorption and emission properties of molecules and molecular complexes [17,18], for example, for improving light-harvesting performance [19,20]. Indeed, if the STM tip and the underlying substrate properties are properly chosen to support nanocavity plasmons (NCP), the plasmonic enhancement can be exploited to unveil the local optical properties of individual molecules upon highly localized excitation of tunneling electrons [13,21–26]. Recently, by utilizing single-molecule manipulation and enhancement in a plasmonic nanocavity, we demonstrated direct real-space visualization of coherent dipole-dipole coupling and associated collective states in constructed molecular dimers [13].

In this work, we construct long nonbonded molecular chains with up to 12 molecules and probe their light emission properties via STM-induced luminescence (STML). By employing subnanometer resolved fluorescence imaging and spectroscopy [13,14,27,28] combined with subnanosecond resolved photon correlation measurements [15,16,29], we demonstrate SPS from the constructed molecular chains and quantitatively explore the influence of the NCP on the SPS behavior for different molecular chain lengths. In particular, we investigate the origin of coherence for the superradiant states and the evolution of spectral shifts, linewidths, and emission intensities.

Figure 1(a) shows the schematic of the STML experiments on an ordered zinc-phthalocyanine (ZnPc) molecular chain by adopting a combined strategy of electronic decoupling and plasmonic enhancement [13,21,23,25,26,30–32]. A silver tip and a silver substrate were used to provide strong emission enhancement by nanocavity plasmons upon proper tuning to resonate with molecular

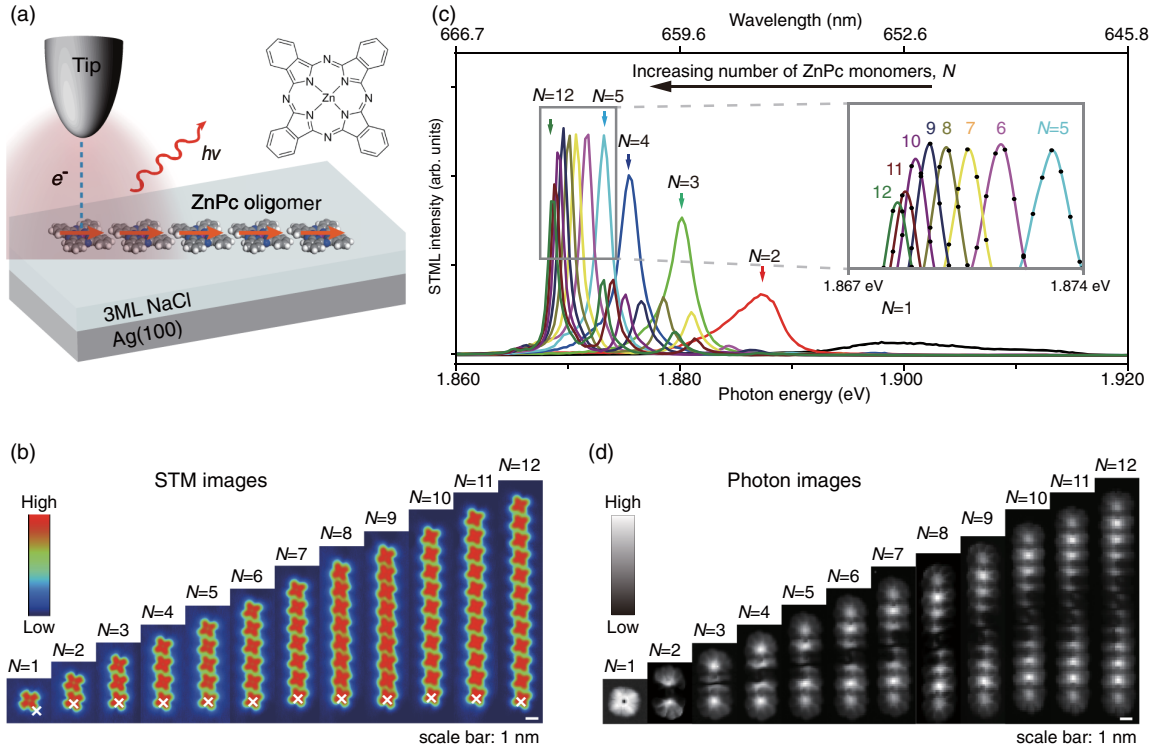

FIG. 1. (a) Schematic of STML from ZnPc molecular chains on NaCl/Ag(100). The nanocavity discussed here refers to the STM junction defined by the STM tip and metal substrate. Inset, ZnPc molecular structure. (b) STM images of ZnPc molecular chains of up to 12 monomers (−2.5 V, 2 pA). (c) Typical STML spectra acquired from different molecular chains by exciting the molecular chains above the positions marked by "×" in (b) (−2.5 V, 200 pA, 20 s). The superradiant peaks of different molecular chains are indicated by arrows. The emergence of the relatively weak high-lying emission peaks (evident here for $N = 6$–12) is associated with other dipole-dipole coupling configurations [13]. (d) Experimental photon images for the superradiant states of the ZnPc chains (−2.5 V, 200 pA, 3 s per pixel).

fluorescence. The experimental methods and conditions are detailed in Sec. S1 of Ref. [33].

In order to explore the spectral evolution of the superradiant states in a systematic manner as a function of the molecular chain length, the numbers of coupled monomers were varied from $N = 2$ to 12 through STM manipulation. Figure 1(b) displays the examples of the STM images of ordered chains with nearest-neighbor molecules in close-contact configuration at a center-to-center distance of ∼1.45 nm. Figure 1(c) shows the evolution of the STML spectra along with increasing N, where the chain was excited at the terminal molecule ($n = 1$) and the luminescence was collected from a diffraction-limited spot by a lens. According to our previous understanding of the coherent intermolecular dipole-dipole coupling [13], the emission peak that is the strongest in intensity and lowest in energy for a given molecular chain length can be assigned to the in-line in-phase superradiant state. Thus, a striking feature of Fig. 1(c) is that superradiant peaks become narrower and redshifted with increasing chain lengths. The $Q(0, 0)$ emission peak for an isolated ZnPc monomer is at ∼1899.6 meV with a linewidth ∼10.8 meV, while the superradiant peak for the molecular chain of $N = 12$ is redshifted to ∼1868.4 meV with a greatly narrowed linewidth ∼1.2 meV (Sec. S2 of Supplemental Material [33]).

In order to visualize how the nanoscopic picture of the intermolecular dipole-dipole coupling evolves in real space with increasing chain lengths, we carried out spatially resolved spectroscopic imaging over each constructed ZnPc chain [13]. In Fig. 1(d), we plot the superradiant emission intensities of a single chain detected in the far field as a function of the location of electronic excitation. The spectroscopic images for the superradiant peaks of ZnPc molecular chains exhibiting centrosymmetric dumbbell-like node patterns are evidently different from that of an isolated ZnPc monomer. To investigate the underlying physics at hand, we performed simulations for molecular chains considering intermolecular dipole-dipole coupling. The very good agreement of the simulated spectroscopic images (Sec. S3 of Supplemental Material [33]) with the experimental photon images in terms of both the positions and numbers of emission nodes and antinodes provides a clear indication of the coherent in-line in-phase intermolecular dipole-dipole coupling over the molecular chains. This in turn supports the assignment of the strongest emission peaks as the superradiant states. In addition,

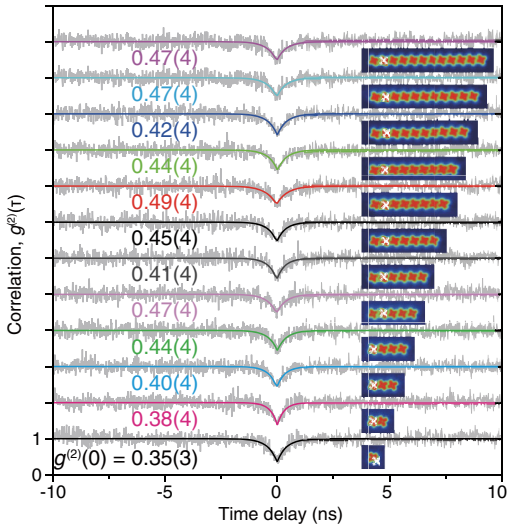

FIG. 2. Second-order correlation functions $g^{(2)}(\tau)$ for different ZnPc chains ($N = 1$–12) (−2.5 V, 200 pA,). The $g^{(2)}(0)$ values for different ZnPc chains are listed. Two factors that cause deviations of $g^{(2)}(0)$ from the ideal value of zero are the temporal resolution of the HBT setup and the fluorescence background from NCP [16].

since the spatially resolved imaging patterns reflect the real-space distribution of photon yields for the superradiant states, the global emission maxima directly reveal the most efficient excitation positions for the controlled generation of such superradiant states, namely, on top of the terminal molecules for $N = 2$–4 and above the molecules next to the terminals for $N = 5$–12.

In order to examine whether the superradiant states of the molecular chains are single-exciton states, we performed photon correlation measurements using a home-built Hanbury Brown–Twiss (HBT) setup to characterize the photon emission statistics [15,16]. Figure 2 shows the second-order correlation function $[g^{(2)}(\tau)]$ measured for the superradiant emission from different ZnPc chains ($N = 1$–12) by positioning the STM tip above the global emission maxima in Fig. 1(d) (also marked by "×" in the inset STM images of Fig. 2) to achieve the strongest emission for each superradiant state. Evident antibunching dips were observed in $g^{(2)}(\tau)$ at zero delay for all molecular chains. As shown in Fig. 2, by fitting the experimental curves with a single exponential function $g^{(2)}(\tau) = 1 - [1 - g^{(2)}(0)]e^{-|\tau|/\tau_0}$ [56], $g^{(2)}(0)$ values were all found to be below the single-photon purity threshold of 0.5 (more details in Sec. S4 of the Supplemental Material [33]), which is a clear indication of single-photon emission [16,57], thus testifying to the occurrence of SPS and the formation of single-exciton superradiant states for molecular chains under localized electronic excitation. We point out in passing that these measurements require an exquisite control over the tip stability for a long time since all the STM manipulation, STML spectra, and HBT measurements for the molecular chains from $N = 2$–12 have to be achieved with the same tip condition.

Notably, the observation of SPS provides a direct experimental proof that a molecular chain with coherent dipole-dipole coupling, once excited, should be treated as a whole and considered as a single quantum system. The picture we have established for the single-exciton superradiant state, a symmetric quantum superposition of products of states of molecular monomers, lays the basis for the quantitative analysis of the spectral evolution of molecular chains in the plasmonic nanocavity, as detailed here (more details in the Supplemental Material [33]).

Previous theoretical studies reported that the presence of plasmonic nanostructures could induce cooperative emission of nearby emitters such as superradiance due to the exchange of virtual plasmons [58,59]. If the NCP played a key role in the generation of superradiance in molecular chains, the coherence length should be similar to the spatial extension of the NCP field (less than 10 nm) [24,60,61]. In other words, once the length of a molecular chain grows beyond the range of the NCP field, one would not expect any discernable spectral shift of the superradiant peak because the monomers positioned outside the NCP field cannot be coupled to other monomers through the NCP. Considering that the chain lengths of ∼10–16 nm for $N = 8$–12 are evidently larger than the spatial extension of the NCP at a STM tip, the experimental observation of a monotonic spectral shift from $N = 2$ to $N = 12$ in Fig. 1(c) and Fig. 3(a) shows that the coherence of the superradiant states in our molecular systems is not dictated by a plasmon-mediated mechanism. In addition, the centrosymmetric dumbbell-like node patterns in the photon images of the superradiant states indicate that the coherent coupling nature is extended to the whole molecular chains for $N = 2$–12 [Fig. 1(d)], regardless of whether the monomers in molecular chains are within or outside the spatial range of the NCP field.

Indeed, the shift of the STML superradiant spectral peaks for different ZnPc chain lengths can be well explained by only considering the intermolecular dipole-dipole coupling model. As shown in Fig. 3(a), the superradiant peaks keep shifting to the red as the chain length increases with respect to the peak position of an isolated ZnPc monomer, but with an ever-decreasing amplitude. The outcome of simulations based on the nearest-neighbor interaction alone predicts such a shift [blue curve in Fig. 3(a)]; however its trend is found to deviate from the experimental data. Considering our previous experimental knowledge that spectral changes can occur for intermolecular distances up to ∼2.8 nm [13] and the fact that the center-to-center distance of the second nearest-neighbor monomers in our constructed molecular chains amounts to ∼2.9 nm, we also explored the interactions among the second nearest-neighbor monomers in a theoretical model. By treating this interaction as a perturbation [33], the outcome of such a calculation [the red curve in Fig. 3(a)]

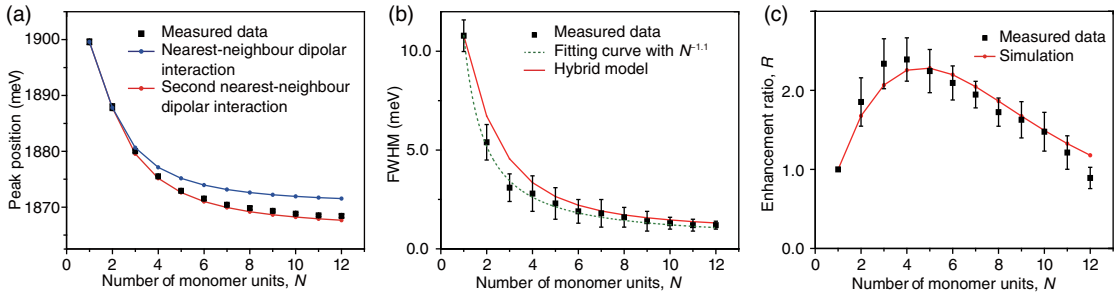

FIG. 3. (a) Spectral shift of the superradiant peaks for different ZnPc chains in STML spectra. (b) Linewidth narrowing of the superradiant peaks for different ZnPc chains obtained from the STML spectra. (c) Emission enhancement ratios R for the superradiant states of molecular chains as a function of N (black squares), calculated by dividing the integrated intensities of the superradiant peaks by that of the monomer emission.

agrees nicely with the experimental data. This lets us conclude that the coherent intermolecular dipole-dipole interaction plays the dominant role in the generation of the superradiant states and the resultant spectral redshifts, overwhelming other contributions of spectral shifting from plasmon-mediated interactions [58] or the collective Lamb shift [62,63] (more details in Sec. S5 of the Supplemental Material [33]).

Although the NCP is not involved in the generation of the superradiant states, the nature of its localized enhancement can modify the emission behavior of a chain, particularly on the spectral linewidth and emission intensity, as illustrated in Figs. 3(b) and 3(c). Figure 3(b) shows that the full width at half-maximum (FWHM) of the superradiant peaks decreases with increasing N (the black squares). The observation of linewidth narrowing is qualitatively similar to that observed in the J-band superradiant peaks of molecular aggregates [8], which has been widely discussed in the context of exchange narrowing models based on either the interaction of identical molecular monomers through vibrations or the statistically distributed electronic energies of rigid molecular monomers [64,65]. Interestingly, all the exchange narrowing models predict an $N^{-0.5}$ relation for the dependence of the linewidth on the number of monomers in a chain [65]. However, the spectral linewidths measured in our case follow an $N^{-1.1}$ trend [green dotted curve in Fig. 3(b)], which is evidently different.

The failure of the exchange narrowing model suggests that the NCP field may play a role in the observed linewidth narrowing. To account for the influence of the inhomogeneous NCP field [illustrated in Fig. 4(a)], we propose a hybrid model by considering both the linewidth contributions from the dephasing [26] that results in the exchange narrowing and the site-dependent decay rates of coupled ZnPc monomers with respect to the position of the STM tip (namely, the plasmonic nanocavity). As detailed in Sec. S3 of the Supplemental Material [33], the linewidth $\Gamma^{\mathrm{tot}}_{\mathrm{sup}}(N)$ of a superradiant peak for a chain with N monomers is the sum of dephasing contributions $\Gamma^{\mathrm{de}}_{\mathrm{sup}}(N)$, the radiative decay rate $\Gamma^{r}_{\mathrm{sup}}(N)$, and nonradiative decay rate $\Gamma^{\mathrm{nr}}_{\mathrm{sup}}(N)$, and it could be expressed as

$$\begin{aligned}\Gamma^{\mathrm{tot}}_{\mathrm{sup}}(N) &= \Gamma^{\mathrm{de}}_{\mathrm{sup}}(N) + \Gamma^{r}_{\mathrm{sup}}(N) + \Gamma^{\mathrm{nr}}_{\mathrm{sup}}(N) \\ &= \sqrt{\sum_{n=1}^{N}(|c_n|^2\Gamma^{\mathrm{de}}_{\mathrm{mono}})^2} + \left|\sum_{n=1}^{N} c_n\sqrt{\Gamma^{r}_{n}}\right|^2 \\ &\quad + \sum_{n=1}^{N}|c_n|^2\Gamma^{\mathrm{nr}}_{n},\end{aligned}$$

where c_n refers to the probability amplitude of the nth monomer for the superradiant state with $|c_n|^2$ standing for the exciton occupation probability, $\Gamma^{\mathrm{de}}_{\mathrm{mono}}$ refers to the dephasing contribution of an isolated ZnPc, and Γ^{r}_{n} (Γ^{nr}_{n}) refers to the radiative (nonradiative) decay rates of an isolated ZnPc placed at the site of the nth monomer. We used electromagnetic simulations to examine the influence of the NCP on the evolution of Γ^{r}_{n} and Γ^{nr}_{n} as a function of the chain length presented in Fig. 4 [33]. As illustrated by

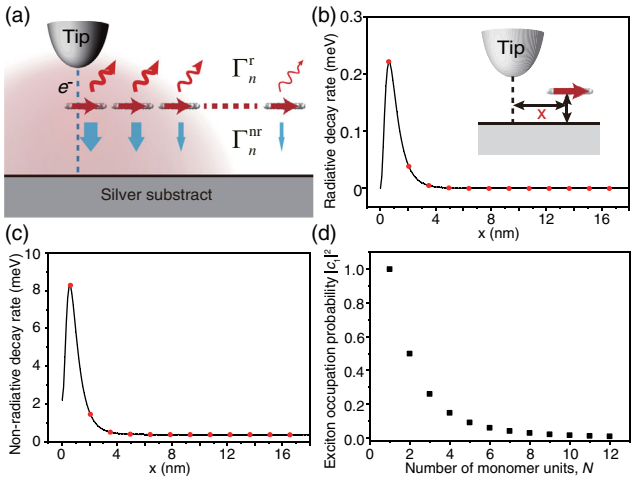

FIG. 4. (a) Schematic showing the decay behavior as a function of the lateral tip-molecule distance due to the inhomogeneous NCP field. (b) Scaled radiative and (c) scaled nonradiative decay rates versus the lateral tip-molecule distances [33]. The inset in (b) shows the schematic of the STM junction for electromagnetic simulations. (d) The evolution of the exciton occupation probabilities for the terminal monomer ($n = 1$) with increasing N.

the red curve in Fig. 3(b), the linewidths calculated by our hybrid model are in fair agreement with the measured data.

To decipher the contributions of radiative and nonradiative decay as well as dephasing to the linewidth, we combined the results of our simulations with the measured Fano spectral features for a monomer as a function of the lateral tip position, as detailed in Sec. S3 of the Supplementary Material [33]. We found that the NCP-enhanced decay rate of ~8.5 meV makes a dominant contribution to the linewidth ~10.8 meV for a single monomer under the STM tip, leaving a minor contribution of ~2.3 meV to arise from dephasing. Thus, the observed linewidth narrowing with increasing N could be roughly understood as follows. As illustrated in Fig. 4(a), different monomers in a molecular chain experience an inhomogeneous electromagnetic environment generated by the highly localized NCP enhancement. For the few molecules close to the tip, both the radiative and nonradiative decay rates are greatly enhanced, making a dominant contribution to the linewidths. The NCP-modified decay rates of the monomers far away from the tip, however, make a minor contribution to the linewidths. In Fig. 1(a), the tip is positioned above a terminal ZnPc monomer ($n = 1$). With increasing chain lengths, the exciton occupation probabilities summed over the ZnPc monomers with broader linewidths close to the tip decrease [exemplified in Fig. 4(d)]. Thus, the total linewidths for the superradiant peaks reduce with increasing N.

The localized NCP enhancement also affects the evolution of the emission intensities for the superradiant peaks of different molecular chains. As shown in Fig. 3(c), the emission intensities first rise with the increase in N, reach a maximum value at about $N \sim 4$ and then decrease with a further increase of N. Such an observation is different from the conventional SPS in atomic systems where the emission intensities are proportional to the number of coupled atoms [11]. As detailed in Ref. [33], the intensity evolution observed here is associated with two factors. First, the coherent in-line in-phase dipole-dipole coupling tends to form a large transition dipole, which would increase the radiative decay rates for the molecular chains in a homogeneous field. Second, only the few monomers underneath the STM tip can make substantial contributions to the emission intensities due to the inhomogeneous NCP enhancement, and this effect decreases upon the growth of the molecular chain because of the decrease of the exciton occupation probabilities for the few monomers under the tip. By taking into account the above factors, the simulated red curve in Fig. 3(c) agrees fairly well with the experimental data, indicating that it is the inhomogeneous NCP enhancement that leads to the deviation from the quasilinear intensity relation predicted for conventional single-exciton superradiant states in a homogeneous field.

We have demonstrated that STML serves as a powerful tool in revealing the underlying physics involved in the optical behavior of molecular collective states and their interaction with NCP. By combining the strategies of STM manipulation, electronic decoupling, and nanocavity plasmonic enhancement with highly localized electron excitation, we realized electrically driven SPS from long entangled molecular chains. The precise spatial control over the molecular arrangement and excitation enables systematic and quantitative investigations of the delocalized molecular collective states in a local plasmonic nanocavity. The nanocavity plasmon is found to have a negligible effect on the intrinsic coherence established by the intermolecular dipole-dipole coupling, but it dramatically modifies the SPS behavior, specifically on linewidth narrowing and intensity evolution. Our findings open up new routes to study molecular energy transfer and quantum many-body physics at the single quantum level.

We thank Professors B. Wang, D. W. Wang, X. G. Li, and C. Lienau for helpful discussions. This work is supported by the National Key R&D Program of China (Grants No. 2016YFA0200600 and No. 2017YFA0303500), the National Natural Science Foundation of China, the Chinese Academy of Sciences, and Anhui Initiative in Quantum Information Technologies. Yang Zhang acknowledges support by Excellent Young Scientist Foundation of the National Natural Science Foundation of China.

*These authors contributed equally to this work.
†Corresponding author.
zhyangnano@ustc.edu.cn
‡Corresponding author.
zcdong@ustc.edu.cn
§Corresponding author.
jghou@ustc.edu.cn

[1] R. H. Dicke, Phys. Rev. **93**, 99 (1954).
[2] C. Hettich, C. Schmitt, J. Zitzmann, S. Kühn, I. Gerhardt, and V. Sandoghdar, Science **298**, 385 (2002).
[3] S. M. Vlaming and A. Eisfeld, J. Phys. D **47**, 305301 (2014).
[4] F. C. Spano and C. Silva, Annu. Rev. Phys. Chem. **65**, 477 (2014).
[5] X. Gao and A. Eisfeld, J. Phys. Chem. Lett. **9**, 6003 (2018).
[6] R. Monshouwer, M. Abrahamsson, F. Van Mourik, and R. Van Grondelle, J. Phys. Chem. B **101**, 7241 (1997).
[7] G. S. Engel, T. R. Calhoun, E. L. Read, T. K. Ahn, T. Mancal, Y. C. Cheng, R. E. Blankenship, and G. R. Fleming, Nature (London) **446**, 782 (2007).
[8] F. Würthner, T. E. Kaiser, and C. R. Saha-Möller, Angew. Chem., Int. Ed. Engl. **50**, 3376 (2011).
[9] S. K. Saikin, A. Eisfeld, S. Valleau, and A. Aspuru-Guzik, Nanophotonics **2**, 21 (2013).
[10] I. Kassal, J. Yuen-Zhou, and S. Rahimi-Keshari, J. Phys. Chem. Lett. **4**, 362 (2013).
[11] M. O. Scully and A. A. Svidzinsky, Science **325**, 1510 (2009).

[12] P. Tighineanu, R. S. Daveau, T. B. Lehmann, H. E. Beere, D. A. Ritchie, P. Lodahl, and S. Stobbe, Phys. Rev. Lett. **116**, 163604 (2016).

[13] Y. Zhang *et al.*, Nature (London) **531**, 623 (2016).

[14] B. Doppagne, M. C. Chong, E. Lorchat, S. Berciaud, M. Romeo, H. Bulou, A. Boeglin, F. Scheurer, and G. Schull, Phys. Rev. Lett. **118**, 127401 (2017).

[15] P. Merino, C. Große, A. Rosławska, K. Kuhnke, and K. Kern, Nat. Commun. **6**, 8461 (2015).

[16] L. Zhang *et al.*, Nat. Commun. **8**, 580 (2017).

[17] S. Kühn, U. Håkanson, L. Rogobete, and V. Sandoghdar, Phys. Rev. Lett. **97**, 017402 (2006).

[18] P. Anger, P. Bharadwaj, and L. Novotny, Phys. Rev. Lett. **96**, 113002 (2006).

[19] O. Andreussi, A. Biancardi, S. Corni, and B. Mennucci, Nano Lett. **13**, 4475 (2013).

[20] E. Wientjes, J. Renger, A. G. Curto, R. Cogdell, and N. F. van Hulst, Nat. Commun. **5**, 4236 (2014).

[21] X. H. Qiu, G. V. Nazin, and W. Ho, Science **299**, 542 (2003).

[22] Z. C. Dong *et al.*, Nat. Photonics **4**, 50 (2010).

[23] H. Imada, K. Miwa, M. Imai-Imada, S. Kawahara, K. Kimura, and Y. Kim, Nature (London) **538**, 364 (2016).

[24] Y. Zhang *et al.*, Nat. Commun. **8**, 15225 (2017).

[25] K. Kuhnke, C. Grosse, P. Merino, and K. Kern, Chem. Rev. **117**, 5174 (2017).

[26] B. Doppagne, M. C. Chong, H. Bulou, A. Boeglin, F. Scheurer, and G. Schull, Science **361**, 251 (2018).

[27] R. Berndt, R. Gaisch, J. K. Gimzewski, B. Reihl, R. R. Schlittler, W. D. Schneider, and M. Tschudy, Science **262**, 1425 (1993).

[28] C. Chen, P. Chu, C. A. Bobisch, D. L. Mills, and W. Ho, Phys. Rev. Lett. **105**, 217402 (2010).

[29] F. Silly and F. Charra, Appl. Phys. Lett. **77**, 3648 (2000).

[30] Z. C. Dong, X. L. Guo, A. S. Trifonov, P. S. Dorozhkin, K. Miki, K. Kimura, S. Yokoyama, and S. Mashiko, Phys. Rev. Lett. **92**, 086801 (2004).

[31] E. Cavar, M. C. Blum, M. Pivetta, F. Patthey, M. Chergui, and W. D. Schneider, Phys. Rev. Lett. **95**, 196102 (2005).

[32] M. C. Chong, G. Reecht, H. Bulou, A. Boeglin, F. Scheurer, F. Mathevet, and G. Schull, Phys. Rev. Lett. **116**, 036802 (2016).

[33] See Supplemental Material at http://link.aps.org/supplemental/10.1103/PhysRevLett.122.233901 for experimental methods, additional experimental data, and more detailed discussion on experimental phenomena and theoretical simulations, which includes Refs. [34–55].

[34] J. Aizpurua, S. P. Apell, and R. Berndt, Phys. Rev. B **62**, 2065 (2000).

[35] G. Hoffmann, J. Aizpurua, P. Apell, and R. Berndt, Surf. Sci. **482–485**, 1159 (2001).

[36] C. Zhang, B. Gao, L. G. Chen, Q. S. Meng, H. Yang, R. Zhang, X. Tao, H. Y. Gao, Y. Liao, and Z. C. Dong, Rev. Sci. Instrum. **82**, 083101 (2011).

[37] D. W. Wang, R. B. Liu, S. Y. Zhu, and M. O. Scully, Phys. Rev. Lett. **114**, 043602 (2015).

[38] M. Kasha, H. R. Rawls, and M. A. El-Bayoumi, Pure Appl. Chem. **11**, 371 (1965).

[39] V. A. Malyshev, J. Lumin. **55**, 225 (1993).

[40] S. W. Wu, G. V. Nazin, and W. Ho, Phys. Rev. B **77**, 205430 (2008).

[41] G. Reecht, F. Scheurer, V. Speisser, Y. J. Dappe, F. Mathevet, and G. Schull, Phys. Rev. Lett. **112**, 047403 (2014).

[42] E. Snoeks, A. Lagendijk, and A. Polman, Phys. Rev. Lett. **74**, 2459 (1995).

[43] H. Imada, K. Miwa, M. Imai-Imada, S. Kawahara, K. Kimura, and Y. Kim, Phys. Rev. Lett. **119**, 013901 (2017).

[44] W. Barnes, J. Mod. Opt. **45**, 661 (1998).

[45] J. M. Hollas, *Modern Spectroscopy* (John Wiley & Sons, West Sussex, 2004).

[46] A. Papoulis and S. U. Pillai, *Probability, Random Variables, and Stochastic Processes* (Tata McGraw-Hill Education, New York, 2002).

[47] A. Eisfeld and J. S. Briggs, Phys. Rev. Lett. **96**, 113003 (2006).

[48] E. W. Knapp, Chem. Phys. **85**, 73 (1984).

[49] M. Sibata, A. Tedesco, and J. Marchetti, European Journal of pharmaceutical sciences **23**, 131 (2004).

[50] T. Feng, Y. Zhou, D. Liu, and J. Li, Opt. Lett. **36**, 2369 (2011).

[51] Y. M. El-Toukhy, M. Hussein, M. F. O. Hameed, A. Heikal, M. Abd-Elrazzak, and S. Obayya, Opt. Express **24**, A1107 (2016).

[52] A. D. Rakić, A. B. Djurišić, J. M. Elazar, and M. L. Majewski, Appl. Opt. **37**, 5271 (1998).

[53] S. Kühn, G. Mori, M. Agio, and V. Sandoghdar, Mol. Phys. **106**, 893 (2008).

[54] E. C. Le Ru and P. G. Etchegoin, *Principles of Surface-Enhanced Raman Spectroscopy* (Elsevier, Amsterdam, 2009).

[55] L. G. Chen, C. Zhang, R. Zhang, X. L. Zhang, and Z. C. Dong, Rev. Sci. Instrum. **84**, 066106 (2013).

[56] P. Michler, A. Imamoğlu, M. Mason, P. Carson, G. Strouse, and S. Buratto, Nature (London) **406**, 968 (2000).

[57] Y. L. A. Rezus, S. G. Walt, R. Lettow, A. Renn, G. Zumofen, S. Gotzinger, and V. Sandoghdar, Phys. Rev. Lett. **108**, 093601 (2012).

[58] V. N. Pustovit and T. V. Shahbazyan, Phys. Rev. Lett. **102**, 077401 (2009).

[59] D. Martín-Cano, L. Martín-Moreno, F. J. García-Vidal, and E. Moreno, Nano Lett. **10**, 3129 (2010).

[60] R. Berndt, R. Gaisch, W. D. Schneider, J. K. Gimzewski, B. Reihl, R. R. Schlittler, and M. Tschudy, Phys. Rev. Lett. **74**, 102 (1995).

[61] M. Barbry, P. Koval, F. Marchesin, R. Esteban, A. Borisov, J. Aizpurua, and D. Sánchez-Portal, Nano Lett. **15**, 3410 (2015).

[62] M. O. Scully, Phys. Rev. Lett. **102**, 143601 (2009).

[63] R. Rohlsberger, K. Schlage, B. Sahoo, S. Couet, and R. Ruffer, Science **328**, 1248 (2010).

[64] M. Wubs and J. Knoester, Chem. Phys. Lett. **284**, 63 (1998).

[65] P. B. Walczak, A. Eisfeld, and J. S. Briggs, J. Chem. Phys. **128**, 044505 (2008).